JACS Au
AN OPEN ACCESS JOURNAL OF THE AMERICAN CHEMICAL SOCIETY

pubs.acs.org/jacsau
Article

Transparent Electrochromic Polymers with High Optical Contrast and Contrast Ratio

Published as part of JACS Au virtual special issue "Polymers for the Clean Energy Transition".

Zhiyang Wang,‡ Liyan You,‡ Vaidehi Pandit, Jagrity Chaudhary, Won-June Lee, and Jianguo Mei*

Cite This: JACS Au 2024, 4, 2291−2299

Read Online

ACCESS | Metrics & More | Article Recommendations | Supporting Information

ABSTRACT: Colored-to-transmissive electrochromic polymers, known for their wide selection of colors and solution processability, have gained great attraction in thin film electrochromic devices that have entered the market. However, their adoption in the real world is limited due to their limited optical transparency and contrast. This study introduces a new molecular design strategy to overcome these issues. This strategy involves using meta-conjugated linkers (MCLs) and aromatic moieties along polymer backbones, which enable transparent-to-colored electrochromic switching. The MCL interrupts charge delocalization, increasing the band gap in the neutral state and ensuring transparency in the visible region. This innovative approach achieves nearly 100% transmittance in the neutral state and a high absorption in the oxidized state, overcoming residue absorption issues in conventional electrochromic polymers. Simultaneously, the MCL and aromatic moieties enable low oxidation potential, facilitating stable transparent-to-color switching. Polymers developed using this approach exhibit wide color tunability, optical contrast exceeding 93%, and cycling stability over 5000 cycles with less than 3% contrast decay. Our research represents a major advancement in overcoming existing challenges, enabling polymer-based electrochromic devices for visual comfort and energy conservation.

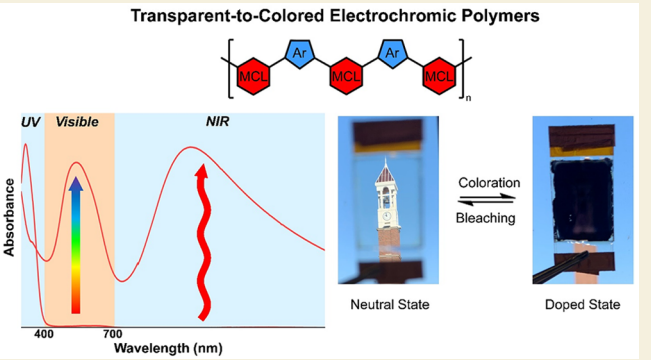

KEYWORDS: *transparent-to-colored polymer, anodically coloring, high optical contrast, contrast ratio, electrochromism*

1. INTRODUCTION

Electrochromic devices (ECDs) allow the dynamic control of light and heat flow and are used in smart windows and glasses,[1−5] biosensors,[6−8] and electronic papers and displays.[9−13] The utilization of electrochromic windows is particularly considered as an efficient energy conservation approach in building efficiency and a critical component in building decarbonization.[14] WO_3-based electrochromic windows have successfully been commercialized by Sage and View,[15] though their market penetration remains low. Compared to inorganic-based vacuum sputtered ECDs, conjugated polymer based ECDs can be manufactured using roll-to-roll coating and lamination.[16] This simple and highly efficient manufacturing process enables the scalable production of large-area and flexible devices with low cost. Ambilight has commercialized large-area roll-to-roll manufactured dynamic smart windows (1.9 m^2) for automotive sunroofs.[17] In conventional conjugated electrochromic polymers (Scheme 1a), the formation of polaron and bipolaron upon electrochemical doping lowers the energy of the optical transition, resulting in red-shift of the absorption from the visible region to the near-IR region and manifesting as colored-to-transmissive change.[18−20] (Scheme 1b) Consequently, their doped state possesses residue absorption throughout the visible region.[21−24] As the film thickness increases, this residue absorption becomes more severe, and the residue color appears.[25,26] (Scheme 1c) Thus, conjugated electrochromic polymers exhibit relatively low optical contrast and contrast ratio, a major factor that limits the further adoption of polymer-based ECDs in applications.

In contrast to conventional conjugated ECPs which undergo colored-to-transmissive change, a reverse design is transparent-to-colored change. These electrochromic materials exhibit higher energy band gaps so that they absorb light in the UV region without any absorption in the visible region in their neutral state, resulting in a completely transparent state. For example, polymers containing chromophore group triarylamine

Received: March 20, 2024
Revised: May 2, 2024
Accepted: May 16, 2024
Published: May 23, 2024

https://doi.org/10.1021/jacsau.4c00254
JACS Au 2024, 4, 2291−2299

Scheme 1. Schematic Illustration of Colored-to-Transmissive and Transparent-to-Colored Electrochromic Polymers[a]

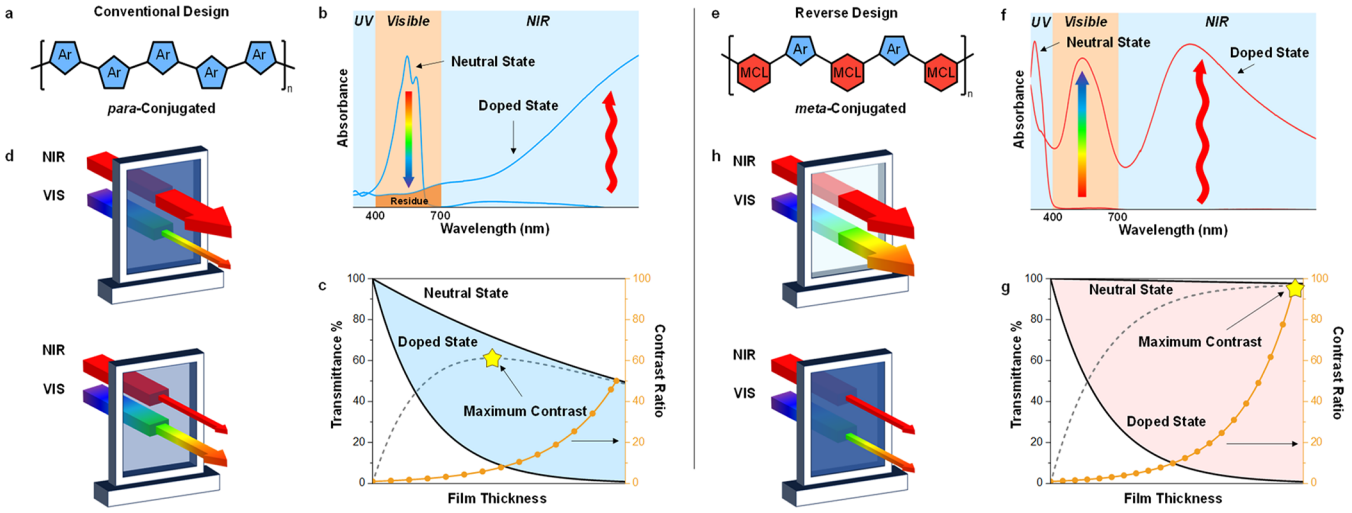

[a](a) Structure of para-conjugated electrochromic polymer. (b) Spectra of the para-conjugated electrochromic polymer in neutral and doped states. (c) Transmittance of para-conjugated electrochromic polymer as a function of thickness. (d) Illustration of the electrochromic window of para-conjugated electrochromic polymer. (e) Structure of meta-conjugated electrochromic polymer. (f) Spectra of the meta-conjugated electrochromic polymer in neutral and doped states. (g) Transmittance of meta-conjugated electrochromic polymer as a function of thickness. (h) Illustration of the electrochromic window of meta-conjugated polymer.

attain transparent-to-colored electrochromic switching.[27−30] Reynolds et al. also reported a series of small molecules based on ethylenedioxythiophene derivatives that can switch from a transparent to a colored state.[31] However, these molecular designs also give rise to specific challenges. First, these polymers usually exhibit limited switching stability. This is due to the fact that the charges formed in the doped state are unable to be delocalized along the polymer chain, resulting in limited stability and durability.[32,33] Second, electrochromic devices based on organic small molecules are usually in the solution/gel phase, hampering the applications in flexible devices. In addition, the color change depends on the diffusion of molecules onto the electrode, thus lacking bistability.

In this study, we report a new design concept for electrochromic polymers that exhibit high transparence in the neutral state while showing high absorption in the oxidized state, leading to the highest optical contrast and contrast ratio ever recorded for EC devices. The design features a polymer backbone consisting of meta-conjugated linkers (MCLs) and aromatic moieties (Scheme 1e). The MCL connects the aromatic moieties at the meta position, interrupting the charge delocalization. Therefore, the band gap of the polymer is enlarged by the presence of meta-conjugation so that the absorption of the neutral polymer could be located in the UV region to achieve a transparent state (Scheme 1f). On the other hand, the MCL and aromatic moieties provide the conjugation to accomplish relatively low oxidation potential for the transparent-to-colored switching which is critical for electrochemical cycling stability. The colors of the polymers can be easily controlled through the selection of MCL and aromatic moieties. We use a series of nine polymers made from three MCLs, carbazole, biphenyl, binaphthanlene, and thiophenes as aromatic moieties, to illustrate this concept and demonstrate versatility of this design. The obtained polymers show a wide color tunability and excellent electrochromic properties. Last, we showcase a neutral gray device made from the blends of these polymers, which boasts an optical contrast of over 93% and a switching stability of more than 5000 cycles with less than 3% contrast decay, highlighting the unmatched potential of this design concept.

2. RESULTS AND DISCUSSION

2.1. Computed Spectroscopic Properties of Meta-conjugated Polymers

Figure 1a details the structures of the meta-conjugated polymers in this study. Each meta-conjugated polymer contains aromatic comonomers which are connected by a MCL at meta-position. We designed a series of polymers containing carbazole (CBZ), biphenyl (BP), and binaphthalene (BNP) as distinct MCLs and a varying number of thiophenes (T1, T2, and T3). In order to guide the experiment and probe the design paradigm from a molecular orbital perspective, density functional theory (DFT) calculations were performed on these meta-conjugated polymers and theoretical spectra were generated for the neutral and radical cation states. Figure 1b depicts the normalized DFT-calculated absorption spectra of CBZ-T1, BP-T1, and BNP-T1 in their neutral states. All three polymers exhibit complete transparency in the visible region, with notable absorption occurring solely in the UV region. While CBZ-T1 and BNP-T1 manifest a slightly red-shifted absorption onset compared to BP-T1, all three polymers maintain absorption wavelengths below 400 nm. In the radical cation states, the absorption in the UV region decreases, leading to an increase in absorption within the visible region (Figure 1c). This transparent-to-colored electrochromism can be further explained by the geometric change of the polymer from neutral to radical cation states. Figure 1d describes polymers' optimized ground state geometries (core part) with different MCLs. DFT calculation suggests that polymers have a completely nonplanar structure in their neutral state with torsional angles around 50° between the MCL and adjacent thiophene (δ_1 and δ_2). This nonplanar structure and significant torsional hindrance impede charge delocalization, increasing the neutral polymer's band gap, so polymer absorbs in sorely in UV region. Whereas, in radical

https://doi.org/10.1021/jacsau.4c00254
JACS Au 2024, 4, 2291−2299

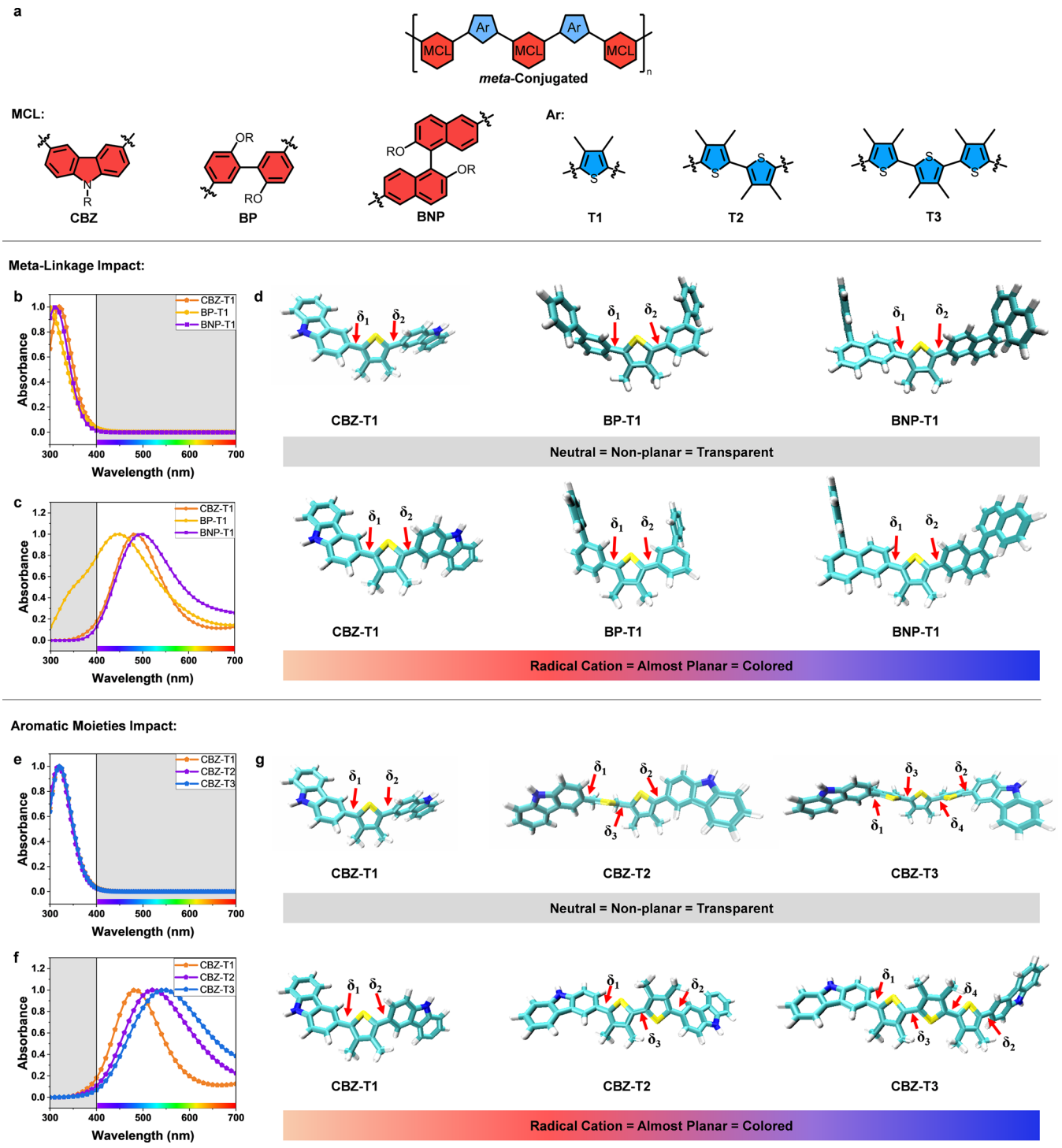

Figure 1. Computed spectroscopic properties of meta-conjugated polymers with (a) three representative MCLs and three aromatic comonomers. Calculated (b) neutral state UV−vis spectra and (c) oxidized state UV−vis spectra of polymers with different MCLs. (d) Optimized backbone geometry of polymers with different MCLs. (e) Neutral state and (f) oxidized state of calculated UV−vis spectra of polymers with different length of aromatic moieties. (g) Optimized backbone geometry of polymers with different length of aromatic moieties.

cation state, the polymer gets planarized with the decrease in torsional angles 25 to 30°, thus charges could delocalize along the polymer chain, and the absorption undergoes a red shift to the visible region for coloration. In contrast with BP-T1, the radical cation absorption of CBZ-T1 and BNP-T1 is more red-shifted due to enlarged conjugation from the CBZ and BNP unit.

We further investigated the impact of the length of aromatic moieties on the optical properties of the polymer (Figure 1e,f). In their neutral states, CBZ-T1, CBZ-T2, and CBZ-T3 exhibit nearly identical absorption spectra, suggesting that the number of thiophene units does not affect the band gap of the polymers. Based on the DFT calculation, the torsional angles between MCL and thiophene remain nearly equivalent across polymers as the number of thiophene increases. In addition,

https://doi.org/10.1021/jacsau.4c00254
JACS Au 2024, 4, 2291−2299

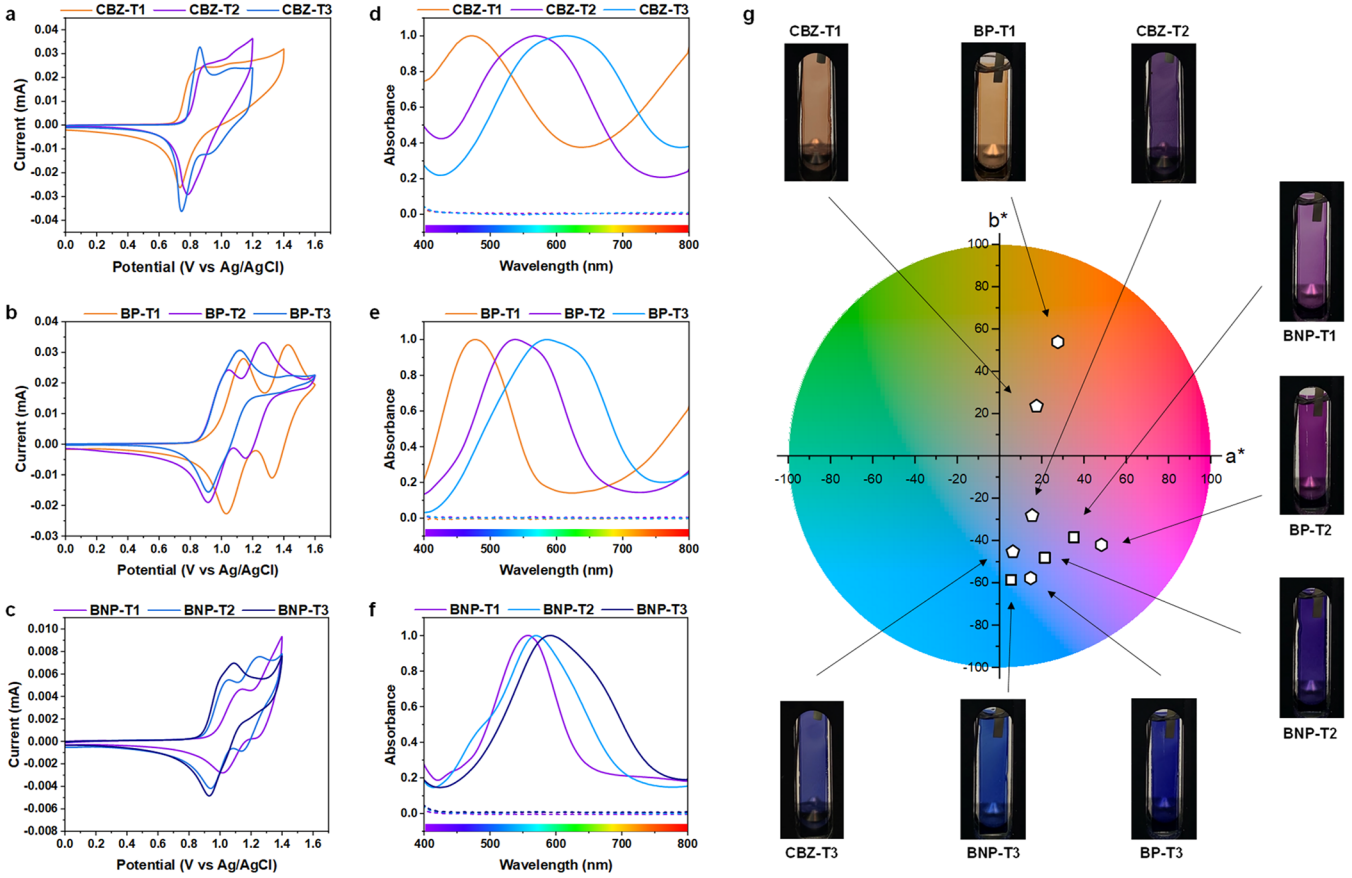

Figure 2. Spectroscopic and electrochemical properties of meta-conjugated polymers. (a–c) CV of CBZ, BP, and BNP polymer solution at scan rate of 20 mV/s. (d–f) spectroscopic properties of CBZ, BP, and BNP polymer thin films in the neutral (dashed) and oxidized (solid) states. (g) CIE $L^*a^*b^*$ color coordinates for all the polymers thin films and their corresponding photographs.

the torsional angles between thiophene units (δ_3 and δ_4) are around 80° which are even larger than the torsional angle between MCL and thiophene. Thus, all polymers exhibit absorption in UV region to achieve transparency. However, in the radical cation state, increasing the number of thiophene units leads to a red shift in the spectra. The absorption peak shifts from 480 to 560 nm from CBZ-T1 to CBZ-T3. Consequently, the radical cation polymers would display distinct colors as we vary the length of aromatic moieties. This color variation can be attributed to the significant torsional angle change when the polymer is oxidized to the radical cation state. Upon oxidation, the torsional angle between each thiophene also decreases to around 25° (Figure 1g), resulting a higher planarity conformation along the polymer backbone. As the aromatic moiety length increases from T1 to T3, the polymer exhibits longer conjugation length, thus rendering a shift in absorption. In general, MCL could hinder the charge delocalization of the neutral polymer and result in complete transparency. The color of the polymer in the radical cation state could be tuned by adjusting the conjugation length of the polymer. The calculated spectra for all the meta-conjugated polymers and torsional angles are available in Figure S11 and Table S2.

2.2. Electrochemical and Spectroscopic Properties of Synthesized Meta-conjugated Polymers

The electrochemical properties of the polymers (see SI for synthesis) are evaluated by cyclic voltammetry (Figure 2a–c) and differential pulse voltammetry (Figure S12), which were performed in the solution phase with 0.2 M $TBAPF_6$/DCM. The cyclic voltammograms display well-resolved quasi-reversible redox process for all meta-conjugated polymers. Upon examination of the polymers via CV, CBZ-T1, CBZ-T2, and CBZ-T3 exhibit one peak indicating the formation of a radical cation. However, polymers containing BP and BNP unit show two redox couples from CV, suggesting the formation of both a radical cation and dication. Comparing the oxidation potential of the polymers with different MCLs, CBZ polymers show the lowest oxidation potential, close to 0.65 V, resulting from the longest conjugation from the carbazole group, followed by 0.75 V for BNP, and 0.8 V for BP polymers. The lowest oxidation onset potential of CBZ polymers is due to the longest conjugation length and the most electron rich nature of the CBZ unit, comparing with BP and BNP units. Besides electrochemistry, the conversion of neutral polymers into the corresponding charged species was also studied in situ by using spectro-electrochemistry in a honeycomb electrode setup (Figure S13). As the applied potential is increased, the absorbance of the neutral polymer in the UV region decreases with the emergence of two peaks in the visible and NIR regions, corresponding to the radical cation. When we further increase the applied potential, particularly the second oxidation peak, the intensity of the peak in the visible region begins to decrease with the continued growth of a broad peak in the NIR region indicative of a dication species. For the BP and BNP polymers, a further increase of the potential would also cause a new absorption peak to form at shorter wavelength (comparing with the NIR absorption), indicating the formation of a dimer

https://doi.org/10.1021/jacsau.4c00254
JACS Au 2024, 4, 2291–2299

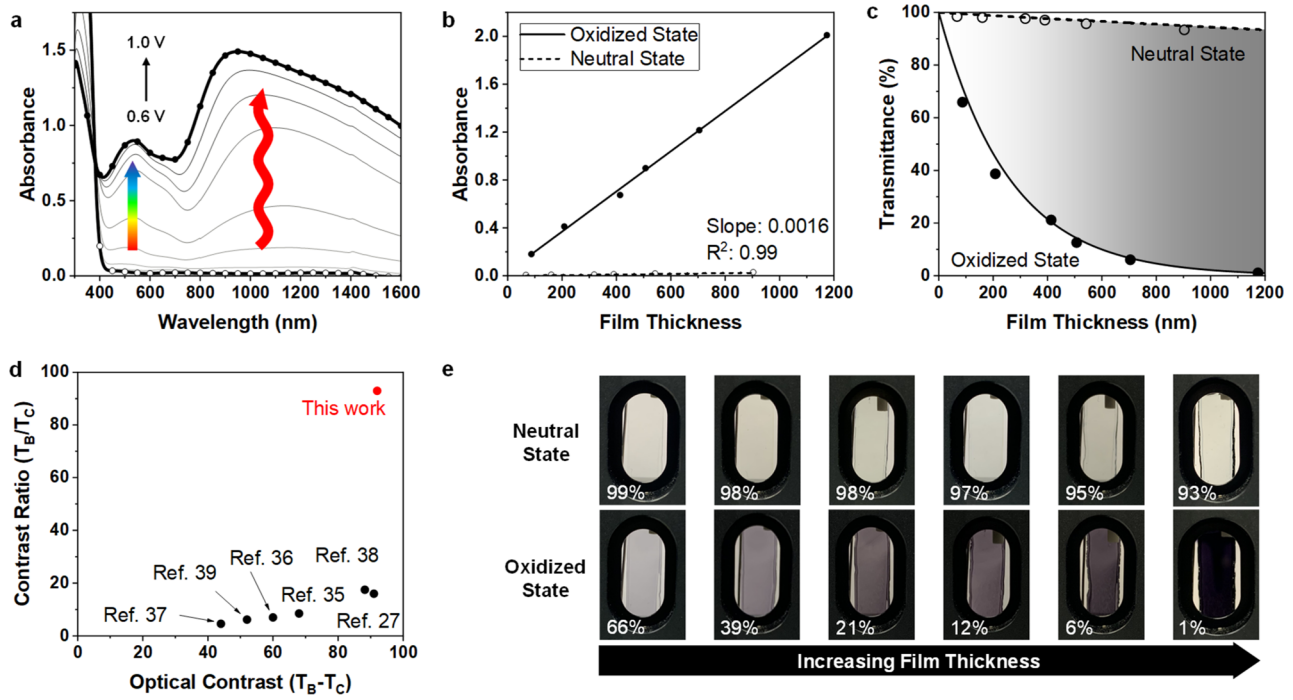

Figure 3. Electrochromic performance of the CBZ-Blend thin film. (a) Spectro-electrochemistry of thin film of CBZ-Blend with 300 nm film thickness at the neutral state. The potential is from 0.6 to 1.0 V with 0.05 V increment versus Ag/AgCl. (b) Beer–Lambert plots of CBZ-Blend in the neutral state (dashed line) and oxidized state (solid) at 550 nm. (c) Transmittance of CBZ-Blend at 550 nm in neutral and oxidized states as a function of film thickness. Experimental results are in dots, and calculated results are in solid and dashed lines. (d) Optical contrast and optical contrast ratio of reported black electrochromic polymers. (e) Photographs of CBZ-Blends at different film thickness in oxidized and neutral states.

dication.[34] It is worth noting that all polymers exhibit relatively low oxidation onset potential, which is attributed to the conjugation from aromatic moieties. The low oxidation onset potential is beneficial for the electrochemical stability of polymers since undesirable side reactions such as water oxidation could be avoided.

Figure 2d–f illustrates the absorption spectra (400–800 nm) of thin films of the meta-conjugated polymers in both their neutral and oxidized states. To conduct the electrochemical and optical measurements, each solution of meta-conjugated polymer was spin-coated onto an ITO glass, serving as the working electrode, and placed in a cuvette. The detailed spectro-electrochemical measurements of each polymer are shown in Figure S14. As a result, meta-conjugated polymers with different lengths of aromatic moieties exhibit distinct colors: orange for T1, purple for T2, and blue for T3 in both BP and CBZ polymers. Figure 2g displays the CIE $L^*a^*b^*$ color coordinates of all the polymers in their oxidized states, along with corresponding thin film photos. Overall, the CBZ polymers exhibit a lower onset potential for oxidation and demonstrate better reversibility at higher potentials. Due to the similarities among the meta-conjugated polymers, our subsequent discussion focuses on the electrochromic properties of CBZ polymers.

2.3. Thin Film Electrochromic Properties

In the field of electrochromics, achieving a transition from neutral gray (black) to transparent is highly desirable in various applications. One strategy to create black color is by combining chromophores with vibrant colors that collectively absorb the entire visible spectrum.[35] Based on this approach, we selected CBZ-T1 (orange) and CBZ-T3 (blue) from our collection of meta-conjugated polymers for blending, aiming to achieve a switch from transparent to black in our electrochromic system. During the blending process, we determined the appropriate ratios of the polymers by considering the absorption coefficients of the polymers in their oxidized states. The Beer–Lambert plots of the polymer films revealed that CBZ-T1 and CBZ-T3 have nearly identical absorption coefficients in their oxidized states (Figure S19), leading us to establish a mass ratio of 1:1 for the CBZ-Blend. Figure 3a illustrates the absorption spectro-electrochemistry of the CBZ-Blend. The neutral film exhibits a transparency range in the visible region, as indicated by its absorption onset at 400 nm. When the CBZ-Blend is oxidized to the radical cation state, it displays two broad absorptions in the visible and near-infrared regions, with peak wavelengths (λ_{max}) at 550 and 950 nm. This demonstrates the synchronized modulation of both light and heat. To investigate the properties of different CBZ-Blend films, we prepared samples with varying thicknesses (Figures S16 and S18) and derived the absorption coefficients through the Beer–Lambert plot (Figure 3b). The neutral (bleached) state absorption coefficient for CBZ-Blend is approximated to be 5×10^2 cm^{-1}, which is 2 orders of magnitude lower than the oxidized (colored) state value, 3.7×10^4 cm^{-1}. It is crucial to acknowledge that our polymer in the neutral state does not exhibit visible light absorption. The measured value, referred to as the "absorption coefficient," does not directly represent the actual polymer absorption. Instead, it serves as an effective coefficient that takes into account the optical losses, such as light scattering or refraction, that occur within films. We utilized the term "absorption coefficient" for the neutral state as a simplification in our explanation.

Beer's Law states that transmittance exponentially decreases with thickness, and the extent of decay is determined by the respective absorption coefficient. By plotting transmittance as a

https://doi.org/10.1021/jacsau.4c00254
JACS Au 2024, 4, 2291–2299

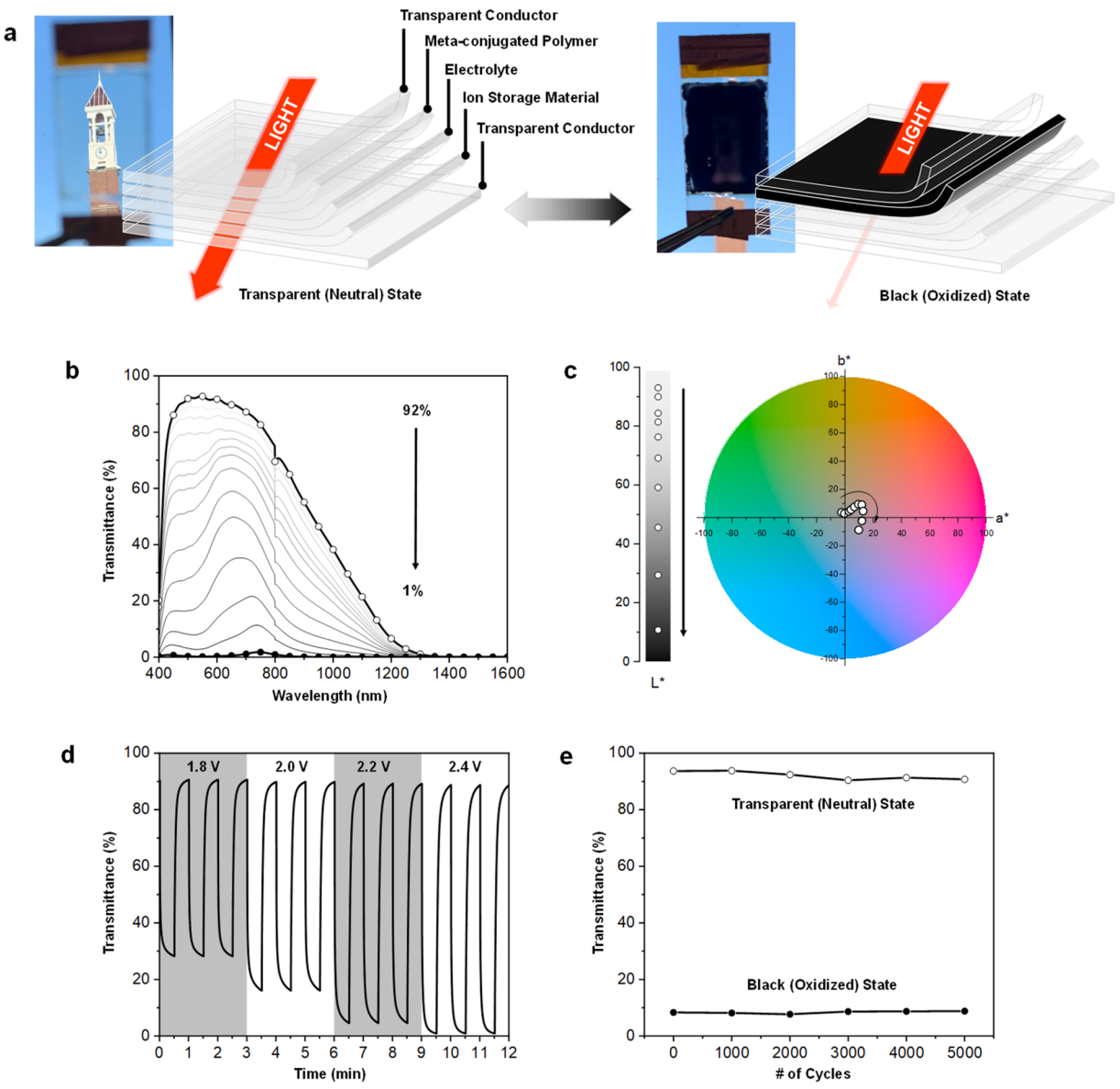

Figure 4. Electrochromic performance of the transparent-to-black solid-state device. (a) Schematic of an electrochromic device. (b) Spectroelectrochemistry of the device. (c) $L^*a^*b^*$ color space of the device. (d) Switching kinetics of the device with different potential ranges. The transmittance is measured at 550 nm. (e) Transmittance of the transparent and black state under 5000 cycles.

function of film thickness using the corresponding α values, we observe that the transmittance remains close to 100% with minimal decay as the film thickness increases in the neutral state, due to its absorption coefficient being close to zero (Figure 3c). Consequently, the optical contrast between the neutral and oxidized states can ideally reach nearly 100%. In addition to optical contrast, the optical contrast ratio, defined as the transmittance ratio between the bleached and colored states, is significant for differentiation between these states. As we increased the film thickness to attain 1% transmittance in the oxidized state, the transmittance in the neutral state remained at 93%, resulting in a high contrast ratio of 93 (Figure 3d,e). Comparative analysis of optical contrast and contrast ratios of various reported black electrochromic polymers shows that the CBZ-Blend outperforms them in terms of its high transmittance in the bleached state.[27,35−39] Furthermore, we gained additional insight into the optical properties of the film by measuring the optical constants (refractive index, n, and extinction coefficient, k) using spectral reflectance combined with optical modeling (Figures S23−S25). The absorption coefficients derived from the optical modeling are consistent with those obtained from the Beer−Lambert plots (Table S4). After demonstrating the remarkable ultrahigh optical contrast for the meta-conjugated electrochromic polymers, we turned our attention to examining the stability of these polymers, specifically their photostability and electrochromic switching stability. To assess their photostability, we subjected the encapsulated polymer film samples to a weathering chamber system equipped with Xenon-arc lamps and a daylight filter that matched the standard air mass (AM) 1.5 illuminant. We measured their absorption spectra and plotted the maximum absorption as a function of irradiation time (Figure S26). In order to evaluate the cycling stability of the thin film polymer, we performed 5000 cyclic voltammetry switching cycles in a 3-electrode setup. The voltage was applied from −0.2 to 1.0 V at a sweep rate of 80

https://doi.org/10.1021/jacsau.4c00254
JACS Au 2024, 4, 2291−2299

mV/s. The transmittance of both the neutral and colored states was recorded at every 1000 cycles (Figure S27). The results showed that the optical contrast of the polymer decreased by only 2%, indicating that the meta-conjugated polymers exhibit suitability for long-term performance.

2.4. Transparent-to-Black Electrochromic Device

The development of electrochromic materials capable of reversible switching between black and transmissive states holds significant importance for various commercial applications. Figure 4a illustrates the configuration of the electrochromic device used in this study. The device was assembled in a two-electrode setup, utilizing CBZ-Blend as the electrochromic layer and nano ITO particles as the ion storage layer (1.5 μm) due to its high transmittance and large charge capacity.[40]

In the spectro-electrochemistry study, the potential of the device was incrementally increased from −0.6 to 2.4 V. As the potential increased, transmittance in the visible region decreased due to the oxidation of CBZ-Blend, resulting in the switch from a transparent state to a black state. The potential was increased until no further changes in transmittance were observed, and the optical contrast between the two states reached 92% (1−93%). The transmittance spectra were referenced to air, encompassing the transmittance loss through the glass, ITO layer, electrolyte layer, and ion storage layer (Figure S28). Taking advantage of the high transparency of the device, the black state transmittance could be simply tuned by the potential applied. As shown in Figure 4d, the black state transmittance decreases from 30% to 1% by increasing the applied potential without the loss in transparent state transmittance and switching speed. The CIE $L^*a^*b^*$ color coordinates at different voltages are depicted in Figure 4c. With an increase in potential, the lightness (L^*) decreased from its initial value of 95 to 10, while the values of a^* and b^* remained close to 0. This indicates a transparent-to-black color switching process without any intermediate colors.

To assess the cycling stability of the device, we performed 5000 cyclic voltammetry switching cycles. The transmittance spectra were measured throughout the cycling process (Figure S29). The transmittance at 550 nm of both the transparent and colored states of the device were plotted in Figure 4e. The optical contrast experienced a slight decrease from its original value of 85% to 81%, which still represents the best cycling stability observed in a black electrochromic device with such a high optical contrast.

3. CONCLUSION

This study presents a novel molecular design by utilizing meta-conjugated linkers (MCL) and aromatic moieties to create electrochromic polymers that undergo transparent-to-colored electrochromic switching. Unlike conventional electrochromic polymers, these new polymers are colorless in their neutral state and highly absorbent in the oxidized state, effectively addressing the limited transparency and contrast issues. The polymers developed through this strategy demonstrate remarkable electrochromic characteristics, including a wide range of color options, extremely high optical contrast and contrast ratio, as well as exceptional cycling stability. Notably, a transparent-to-black electrochromic device has been successfully achieved through polymer blending, showcasing an optical contrast surpassing 92% and a contrast ratio of 93. These achievements establish a new benchmark in black electrochromics and signify a significant advancement in the field of polymer-based electrochromic devices.

4. EXPERIMENTAL SECTION

4.1. Materials

Tetrabutylammonium hexafluorophosphate ($TBAPF_6$), bis-(trifluoromethane)sulfonimide lithium salt (LiTFSI), dichloromethane (DCM), propylene carbonate (PC, anhydrous, 99.7%), poly(ethylene glycol) diacrylate (PEGDA, average M_n 700), 2-hydroxy-2-methylpropiophenone (HMP), indium tin oxide dispersion (<100 nm particle size (DLS), 30 wt % in isopropanol) were purchased from Sigma-Aldrich. Isopropanol (IPA) and chloroform were purchased from Fisher Scientific. All chemicals were used as received. All electrolytes were made in a nitrogen-filled glovebox.

4.2. Polymer Solution Characterization

Solution phase electrochemical experiments were measured using three-electrode setup in $TBAPF_6$ (0.2 M) in DCM as the supporting electrolyte. The tested polymers were dissolved in DCM at 5 mM. The three-electrode cell consisted of a platinum wire counter electrode, a platinum button working electrode, and a leakless Ag/AgCl reference electrode (eDAQ). The surface of the working electrode was polished with 0.3 um alumina. Cyclic voltammetry (CV) and differential pulse voltammetry (DPV) were performed using Biologic SP150 potentiostat and analyzed using EC-Lab software. In-situ spectro-electrochemical characterizations were carried out in a cuvette of 1 mm path length using a platinum honeycomb-electrode (Pine Research) with a built-in counter electrode. An identical cuvette and honeycomb-electrode with electrolyte was used as reference. The same Ag/AgCl reference electrode used for the CV and DPV measurements were used in these experiments. The absorptions were measured using a Cary 5000 UV−vis spectrometer.

4.3. Thin Film Preparation and Characterization

The polymers were dissolved in chloroform at specific concentrations and filtered through a 0.45 μm filter for later thin film preparation. ITO-glass substrates (50 mm × 7 mm × 0.5 mm) were cleaned by sonicating the in acetone for 15 min then IPA for 15 min before drying in an oven. Thin films were prepared by spin coating 0.1 mL of the polymer solution onto an ITO substrate at a speed of 1500 rpm for 1 min using a Laurell spin coater. The film thickness was measured using a Veeco dimension 3100 atomic force microscopy (AFM).

The electrochemical experiments were carried out in a cuvette consisting of polymer coated ITO as working electrode, a leakless Ag/AgCl reference electrode, Pt wire as the counter electrode and 0.2 M LiTFSI in PC as supporting electrolyte. A bare ITO/glass substrate in an identical cuvette filled with the same electrolyte was used to collect baseline of the measurements. The electrochromic performance of polymer thin films were tested using the following procedure. The polymer thin films were first electrochemically conditioned by chronoamperometry (CA) at 1 V until the entire film could change color uniformly. The absorption profile of the oxidized (colored) and neutral (transparent) state films were recorded while applying a potential of 1 and −0.4 V, respectively. The switching kinetics of the polymer films were measured through stepwise potential fast chronoamperometry (SPFC) by applying oxidizing and reducing potentials for 60 s each and recording the transmittance changes in situ at λ_{max} of the polymer. The long-term cycling of CBZ-Blend was performed using SPFC in a Faraday cage under ambient conditions.

To obtain the absorption coefficient of each polymer, the absorptions at neutral and oxidized states were measured and plotted against different film thickness. A linear fit of five points was used to obtain the slope and multiplied by a factor of 2.303 to calculate the absorption coefficient. The thickness for the neutral state film was assumed to be similar to that of the pristine film. A swelling factor of 17%, 40%, 40%, and 30% were assumed for the oxidized state films of CBZ-T1, CBZ-T2, CBZ-T3, and CBZ-Blend, respectively, according to the spectral reflectance measurement.

https://doi.org/10.1021/jacsau.4c00254
JACS Au 2024, 4, 2291−2299

4.4. Photostability Test of Polymer Thin Films

In accordance with the previously described method for preparing polymer thin films, each polymer solution was applied onto ITO-glass substrates (30 mm × 50 mm × 0.7 mm) to prepare the polymer films. Subsequently, within a nitrogen-filled inert atmosphere glovebox (O_2 and H_2O < 1 ppm at 25 °C), the polymer-coated surface was placed facing a cleaned slide glass (50 mm × 75 mm × 1 mm, Corning Inc.). A UV-curable epoxy encapsulant (XNR5516Z, Nagase ChemteX Co., Ltd., Japan) was then adequately applied to the edges of the ITO glass substrate, followed by curing under a UV lamp for 15 min. After encapsulation, the samples were sequentially transferred to a weathering chamber system equipped with three 1800 W xenon arc lamps and a daylight-Q filter (Q-SUN Xe-3, Q-Lab Co., USA). This setup was designed to stably provide light irradiation simulating the AM 1.5 solar spectrum and maximum reference daylight with a xenon-arc standard intensity of 1000 W/m^2 (narrow band irradiance control at 0.51 W/m^2/nm at 340 nm). The samples were exposed to light for durations of 24, 48, 72, 96, 120, 144, and 168 h, positioning an uncoated glass cover slide toward the lamp. During the light exposure, the chamber's internal temperature was maintained at 55 °C to counteract any temperature increase caused by the Xe-lamps. A standard sample, also encapsulated, was exposed to the same conditions as a baseline for comparison and characterization.

4.5. Spectral Reflectance Measurement

Thin films of each polymer were spin coated on ITO-glass (30 mm × 25 mm × 0.7 mm) and were electrochemically oxidized or reduced in 0.2 M LiTFSI in PC using chronoamperometry to obtain oxidized and neutral state films, respectively. The films were blow-dried under nitrogen gas, and the transmittance and reflectance were measured by F10-RT-EXR (Filmetrics). Spectra for bare ITO glass was also measured for purposes of optical modeling. The transmittance and reflectance spectra were fitted using WVASE ellipsometric software to calculate n and k values.

4.6. Device Fabrication and Characterization

The electrochromic devices were assembled using polymers as the anode (working electrode), ITO nanoparticles as the counter electrode (cathode), and PEGDA/LiTFSI as the gel electrolyte. An 80 mg/mL ECP-Blend solution in chloroform was prepared and spin coated onto ITO glass substrate (30 mm × 25 mm × 0.7 mm) at a speed of 1500 rpm as the anode. To prepare the cathode, the ITO dispersion was spin coated onto an ITO glass substrate at 1000 rpm; this process was repeated 1 more time for the second layer. The cathode was then annealed at 200 °C for 1 h to remove the solvent. The gel electrolyte was prepared by mixing PEGDA, 0.2 M LiTFSI/PC, and HMP in a volume ratio of 5:5:1, respectively. The gel electrolyte was drop-casted onto the anode, and then the cathode was placed on top of the electrolyte. The device was irradiated under a UV lamp (SUNUV, 24W) for 10 min to induce cross-linking of PEGDA. The electrochromic performance of the device was tested following the same procedure as thin film characterization, except the long-term cycling stability, which was tested by a CHI 660E potentiostat and Ocean Optics spectrometer in a nitrogen filled glovebox.

■ ASSOCIATED CONTENT

Supporting Information

The Supporting Information is available free of charge at https://pubs.acs.org/doi/10.1021/jacsau.4c00254.

Methods, polymer synthesis, polymer characterization, DFT calculations, polymer solution electrochemical and optical characterization, thin film characterization, optical modeling, thin film stability, device performance (PDF)

Video of the ECD (MP4)

■ AUTHOR INFORMATION

Corresponding Author

Jianguo Mei − *Department of Chemistry, Purdue University, West Lafayette, Indiana 47907, United States;* orcid.org/0000-0002-5743-2715; Email: jgmei@purdue.edu

Authors

Zhiyang Wang − *Department of Chemistry, Purdue University, West Lafayette, Indiana 47907, United States*

Liyan You − *Department of Chemistry, Purdue University, West Lafayette, Indiana 47907, United States*

Vaidehi Pandit − *Department of Chemistry, Purdue University, West Lafayette, Indiana 47907, United States*

Jagrity Chaudhary − *Department of Chemistry, Purdue University, West Lafayette, Indiana 47907, United States*

Won-June Lee − *Department of Chemistry, Purdue University, West Lafayette, Indiana 47907, United States;* orcid.org/0000-0001-8756-0956

Complete contact information is available at: https://pubs.acs.org/10.1021/jacsau.4c00254

Author Contributions

‡Z.W. and L.Y. contributed equally to this work. J. M. conceived the idea of this study. L.Y. and J.M. designed the polymers. Z.W. performed materials characterizations and device fabrications. L.Y. and V.P synthesized the polymers. J.C. performed DFT calculations. W.L. performed weathering experiments and instrumental analysis. Z.W. and J.M. drafted the manuscript.

Funding

Ambilight Inc., Research contract: #4000187.02.

Notes

The authors declare the following competing financial interest(s): Jianguo Mei is a co-founder of Ambilight Inc, which financially sponsors this research.

■ ACKNOWLEDGMENTS

We acknowledge financial support from Ambilight Inc. under research contract Grant #4001872.02. We also thank Kuluni Perera, Ke Chen, Kai Lang, and Jianing Zhou for their assistance.

■ REFERENCES

(1) Kim, Y.; Han, M.; Kim, J.; Kim, E. Electrochromic Capacitive Windows Based on All Conjugated Polymers for a Dual Function Smart Window. *Energy Environ. Sci.* **2018**, *11* (8), 2124−2133.

(2) Kim, J.; Rémond, M.; Kim, D.; Jang, H.; Kim, E. Electrochromic Conjugated Polymers for Multifunctional Smart Windows with Integrative Functionalities. *Adv. Mater. Technol.* **2020**, *5* (6), 1900890.

(3) Azens, A.; Granqvist, C. Electrochromic Smart Windows: Energy Efficiency and Device Aspects. *J. Solid State Electrochem.* **2003**, *7* (2), 64−68.

(4) Runnerstrom, E. L.; Llordés, A.; Lounis, S. D.; Milliron, D. J. Nanostructured Electrochromic Smart Windows: Traditional Materials and NIR-Selective Plasmonic Nanocrystals. *Chem. Commun.* **2014**, *50* (73), 10555−10572.

(5) Lin, S.; Bai, X.; Wang, H.; Wang, H.; Song, J.; Huang, K.; Wang, C.; Wang, N.; Li, B.; Lei, M.; Wu, H. Roll-to-Roll Production of Transparent Silver-Nanofiber-Network Electrodes for Flexible Electrochromic Smart Windows. *Adv. Mater.* **2017**, *29* (41), 1703238.

(6) Ranjbar, S.; Nejad, M. A. F.; Parolo, C.; Shahrokhian, S.; Merkoçi, A. Smart Chip for Visual Detection of Bacteria Using the

Electrochromic Properties of Polyaniline. *Anal. Chem.* **2019**, *91* (23), 14960−14966.
(7) Yu, Z.; Cai, G.; Liu, X.; Tang, D. Pressure-Based Biosensor Integrated with a Flexible Pressure Sensor and an Electrochromic Device for Visual Detection. *Anal. Chem.* **2021**, *93* (5), 2916−2925.
(8) Farahmand Nejad, M. A.; Ranjbar, S.; Parolo, C.; Nguyen, E. P.; Álvarez-Diduk, R.; Hormozi-Nezhad, M. R.; Merkoçi, A. Electrochromism: An Emerging and Promising Approach in (Bio)Sensing Technology. *Mater. Today* **2021**, *50*, 476−498.
(9) Yin, L.; Cao, M.; Kim, K. N.; Lin, M.; Moon, J.-M.; Sempionatto, J. R.; Yu, J.; Liu, R.; Wicker, C.; Trifonov, A.; Zhang, F.; Hu, H.; Moreto, J. R.; Go, J.; Xu, S.; Wang, J. A Stretchable Epidermal Sweat Sensing Platform with an Integrated Printed Battery and Electrochromic Display. *Nat. Electron.* **2022**, *5* (10), 694−705.
(10) Howard, E. L.; Österholm, A. M.; Shen, D. E.; Panchumarti, L. P.; Pinheiro, C.; Reynolds, J. R. Cost-Effective, Flexible, and Colorful Dynamic Displays: Removing Underlying Conducting Layers from Polymer-Based Electrochromic Devices. *ACS Appl. Mater. Interfaces* **2021**, *13* (14), 16732−16743.
(11) Wang, Y.; Nie, H.; Han, J.; An, Y.; Zhang, Y.-M.; Zhang, S. X.-A. Green Revolution in Electronic Displays Expected to Ease Energy and Health Crises. *Light Sci. Appl.* **2021**, *10* (1), 33.
(12) Matsuhisa, N.; Niu, S.; O'Neill, S. J. K.; Kang, J.; Ochiai, Y.; Katsumata, T.; Wu, H.-C.; Ashizawa, M.; Wang, G.-J. N.; Zhong, D.; Wang, X.; Gong, X.; Ning, R.; Gong, H.; You, I.; Zheng, Y.; Zhang, Z.; Tok, J. B.-H.; Chen, X.; Bao, Z. High-Frequency and Intrinsically Stretchable Polymer Diodes. *Nature* **2021**, *600* (7888), 246−252.
(13) Yan, C.; Kang, W.; Wang, J.; Cui, M.; Wang, X.; Foo, C. Y.; Chee, K. J.; Lee, P. S. Stretchable and Wearable Electrochromic Devices. *ACS Nano* **2014**, *8* (1), 316−322.
(14) Hee, W. J.; Alghoul, M. A.; Bakhtyar, B.; Elayeb, O.; Shameri, M. A.; Alrubaih, M. S.; Sopian, K. The Role of Window Glazing on Daylighting and Energy Saving in Buildings. *Renew. Sustain. Energy Rev.* **2015**, *42*, 323−343.
(15) Sbar, N.; Badding, M.; Budziak, R.; Cortez, K.; Laby, L.; Michalski, L.; Ngo, T.; Schulz, S.; Urbanik, K. Progress toward Durable, Cost Effective Electrochromic Window Glazings. *Sol. Energy Mater. Sol. Cells* **1999**, *56* (3), 321−341.
(16) Jensen, J.; Hösel, M.; Dyer, A. L.; Krebs, F. C. Development and Manufacture of Polymer-Based Electrochromic Devices. *Adv. Funct. Mater.* **2015**, *25* (14), 2073−2090.
(17) Gu, C.; Jia, A.-B.; Zhang, Y.-M.; Zhang, S. X.-A. Emerging Electrochromic Materials and Devices for Future Displays. *Chem. Rev.* **2022**, *122* (18), 14679−14721.
(18) Patil, A. O.; Heeger, A. J.; Wudl, F. Optical Properties of Conducting Polymers. *Chem. Rev.* **1988**, *88* (1), 183−200.
(19) Bredas, J. L.; Street, G. B. Polarons, Bipolarons, and Solitons in Conducting Polymers. *Acc. Chem. Res.* **1985**, *18* (10), 309−315.
(20) Tolbert, L. M. Solitons in a Box: The Organic Chemistry of Electrically Conducting Polyenes. *Acc. Chem. Res.* **1992**, *25* (12), 561−568.
(21) Osterholm, A. M.; Nhon, L.; Shen, D. E.; Dejneka, A. M.; Tomlinson, A. L.; Reynolds, J. R. Conquering Residual Light Absorption in the Transmissive States of Organic Electrochromic Materials. *Mater. Horiz.* **2022**, *9* (1), 252−260.
(22) Christiansen, D. T.; Wheeler, D. L.; Tomlinson, A. L.; Reynolds, J. R. Electrochromism of Alkylene-Linked Discrete Chromophore Polymers with Broad Radical Cation Light Absorption. *Polym. Chem.* **2018**, *9* (22), 3055−3066.
(23) Nhon, L.; Wilkins, R.; Reynolds, J. R.; Tomlinson, A. Guiding Synthetic Targets of Anodically Coloring Electrochromes through Density Functional Theory. *J. Chem. Phys.* **2021**, *154* (5), 054110.
(24) Bubnova, O.; Crispin, X. Towards Polymer-Based Organic Thermoelectric Generators. *Energy Environ. Sci.* **2012**, *5* (11), 9345−9362.
(25) Padilla, J.; Österholm, A. M.; Dyer, A. L.; Reynolds, J. R. Process Controlled Performance for Soluble Electrochromic Polymers. *Sol. Energy Mater. Sol. Cells* **2015**, *140*, 54−60.
(26) Li, X.; Perera, K.; He, J.; Gumyusenge, A.; Mei, J. Solution-Processable Electrochromic Materials and Devices: Roadblocks and Strategies towards Large-Scale Applications. *J. Mater. Chem. C* **2019**, *7* (41), 12761−12789.
(27) Zhang, Q.; Tsai, C.-Y.; Li, L.-J.; Liaw, D.-J. Colorless-to-Colorful Switching Electrochromic Polyimides with Very High Contrast Ratio. *Nat. Commun.* **2019**, *10* (1), 1239.
(28) Shao, M.; Lv, X.; Zhou, C.; Ouyang, M.; Zhu, X.; Xu, H.; Feng, Z.; Wright, D. S.; Zhang, C. A Colorless to Multicolored Triphenylamine-Based Polymer for the Visualization of High-Performance Electrochromic Supercapacitor. *Sol. Energy Mater. Sol. Cells* **2023**, *251*, 112134.
(29) Zeng, J.; Yang, H.; Zhong, C.; Rajan, K.; Sagar, R. U. R.; Qi, X.; Deng, Y.; Jiang, H.; Liu, P.; Liang, T. Colorless-to-Black Electrochromic Devices Based on Ambipolar Electrochromic System Consisting of Cross-Linked Poly(4-Vinyltriphenylamine) and Tungsten Trioxide with High Optical Contrast in Visible and near-Infrared Regions. *Chem. Eng. J.* **2021**, *404*, 126402.
(30) Zhang, K.; Niu, H.; Wang, C.; Bai, X.; Lian, Y.; Wang, W. Novel Aromatic Polyimides with Pendent Triphenylamine Units: Synthesis, Photophysical, Electrochromic Properties. *J. Electroanal. Chem.* **2012**, *682*, 101−109.
(31) Christiansen, D. T.; Tomlinson, A. L.; Reynolds, J. R. New Design Paradigm for Color Control in Anodically Coloring Electrochromic Molecules. *J. Am. Chem. Soc.* **2019**, *141* (9), 3859−3862.
(32) Zhang, L.; Luo, F.; Li, W.; Yan, S.; Chen, Z.; Zhao, R.; Ren, N.; Wu, Y.; Chen, Y.; Zhang, C. Conjugation-Broken Thiophene-Based Electropolymerized Polymers with Well-Defined Structures: Effect of Conjugation Lengths on Electrochromic Properties. *Phys. Chem. Chem. Phys.* **2019**, *21* (43), 24092−24100.
(33) Cao, K.; Shen, D. E.; Österholm, A. M.; Kerszulis, J. A.; Reynolds, J. R. Tuning Color, Contrast, and Redox Stability in High Gap Cathodically Coloring Electrochromic Polymers. *Macromolecules* **2016**, *49* (22), 8498−8507.
(34) Perera, K.; Wu, W.; Jenkins, K. A.; Espenship, M. F.; Zeller, M.; You, L.; Ahmed, M.; Lang, K.; Liu, G.; Chaudhary, J.; Abtahi, A.; Forbes, D.; Laskin, J.; Savoie, B. M.; Mei, J. Degradation Pathways of Conjugated Radical Cations. *Chem. Mater.* **2023**, *35* (21), 9135−9149.
(35) Savagian, L. R.; Österholm, A. M.; Shen, D. E.; Christiansen, D. T.; Kuepfert, M.; Reynolds, J. R. Conjugated Polymer Blends for High Contrast Black-to-Transmissive Electrochromism. *Adv. Opt. Mater.* **2018**, *6* (19), 1800594.
(36) Kerszulis, J. A.; Bulloch, R. H.; Teran, N. B.; Wolfe, R. M. W.; Reynolds, J. R. Relax: A Sterically Relaxed Donor-Acceptor Approach for Color Tuning in Broadly Absorbing, High Contrast Electrochromic Polymers. *Macromolecules* **2016**, *49* (17), 6350−6359.
(37) Lo, C. K.; Shen, D. E.; Reynolds, J. R. Fine-Tuning the Color Hue of π-Conjugated Black-to-Clear Electrochromic Random Copolymers. *Macromolecules* **2019**, *52* (17), 6773−6779.
(38) Sun, N.; Su, K.; Zhou, Z.; Wang, D.; Fery, A.; Lissel, F.; Zhao, X.; Chen, C. Colorless-to-Black" Electrochromic and AIE-Active Polyamides: An Effective Strategy for the Highest-Contrast Electrofluorochromism. *Macromolecules* **2020**, *53* (22), 10117−10127.
(39) Wang, Z.; Andjaba, J. M.; Rybak, C.; You, L.; Uyeda, C.; Mei, J. Black-to-Transmissive Dual Polymer Complementary Electrochromics with High Coloration Efficiency. *Chem. Eng. J.* **2023**, *456*, 141013.
(40) Shen, D. E.; Iyer, D. B.; Dejneka, A. M.; Reynolds, J. R.; Österholm, A. M. Mesoporous ITO Electrodes as Optically Passive Counter Electrodes for Electrochromic Devices. *ACS Appl. Opt. Mater.* **2023**, *1* (4), 906−914.

NOTE ADDED AFTER ASAP PUBLICATION

This paper was published ASAP on May 23, 2024, with errors in Figure 1. These were corrected in the version published ASAP on May 28, 2024.

https://doi.org/10.1021/jacsau.4c00254
JACS Au 2024, 4, 2291−2299